PCCP

High-temperature 2D ferromagnetism in conjugated microporous porphyrin-type polymers

Journal:	*Physical Chemistry Chemical Physics*
Manuscript ID	CP-ART-04-2020-002312.R1
Article Type:	Paper
Date Submitted by the Author:	11-Jun-2020
Complete List of Authors:	Pimachev, Artem; University of Colorado Boulder, Aerospace Mechanics Research Nielsen, Robert; University of Wyoming, Physics and Astronomy Dahnovsky, Yuri; University of Wyoming, Physics and Astronomy

High-temperature 2D ferromagnetism in conjugated microporous porphyrin-type polymers.

Artem Pimachev

Aerospace Mechanics Research Center

University of Colorado Boulder

Boulder, CO 80309

Robert D. Nielsen and Yuri Dahnovsky

Department of Physics and Astronomy/3905

1000 E. University Avenue

University of Wyoming

Laramie, WY 82071

(Dated: June 11, 2020)

Abstract

The need for magnetic 2D materials that are stable to the enviroment and have high Curie temperatures are very important for various electronic and spintronic applications. We have found that two-dimensional porphyrin-type aza-conjugated microporous polymer crystals are such a material (Fe-aza-CMPs). Fe-aza-CMPs are stable to CO, CO_2, and O_2 atmospheres and show unusual adsorption, electronic, and magnetic properties. Indeed, they are semiconductors with small energy band gaps ranging from 0.27 eV to 0.626 eV. CO, CO_2, and O_2 molecules can be attached in three different ways where single, double, or triple molecules are bound to iron atoms in Fe-aza-CMPs. For different attachment configurations we find that for CO and CO_2 a uniform distribution of the molecules is most energetically favorable while for O_2 molecules aggregation is most energetically preferable. The magnetic moments decrease from 4 to 2 to 0 for singly, doubly, triply occupied configurations for all gasses respectively. The most interesting magnetic properties are found for O_2 molecules attached to the Fe-aza-CMP. For a single attachment configuration we find that an antiferromagnetic state is favorable. When two O_2 molecules are attached, the calculations show the highest exchange integral with a value of $J = 1071\ \mu eV$. This value has been verified by two independent methods where in the first method J is calculated by the energy difference between ferromagnetic and anitferromagnetic configurations. The second method is based on the frozen magnon approach where the magnon dispersion curve has been fitted by the Ising model. For the second method J has been estimated at $J = 1100\ \mu eV$ in excelleent agreement with the first method.

I. INTRODUCTION

Two-dimensional (2D) materials offer unique technological applications due to their unusual electronic, electron transport, optical, and magnetic properties.[1–3] Recently, the discovery of magnetism in 2D crystals presents interesting opportunities for 2D magnetic, magneto-electric and magneto-optic devices.[4,5] However, 2D crystal materials with intrinsic magnetic and electronic properties are difficult to make at room temperatures. For example, ferromagnetic (FM) transition-metal dichalcogenides (TMDCs) are metallic in nature[6], while only some types of 2D materials are semiconductors. Indeed, transition-metal trichalcogenides (TMTCs) $CrXTe_3$ (X = Si, Ge and Sn)[7,8] and chromiumtrihalides CrA_3 (A = F, Cl, Br and I)[9] have been reported as intrinsic FM semiconducting materials. Such materials are toxic and unstable in open air, breaking down in several minutes modifying their physical properties.[10]

In this work we study 2D organic porphyrin-type ferromagnetic semiconductors based on π-conjugated microporous polymers (CMPs) with different gas molecules (CO, CO_2, and O_2) attached to the iron atoms. The choice of the selected gas molecules is natural in biological applications because red blood cells easily attract and release CO, CO_2, and O_2 in biological activities. The study of their physical properties allows us to understand how these gases attach and dispatch in living organisms. Moreover, we propose how to determine the concentration of gasses using their electron transport, optical, and magnetic properties. The magnetic properties are also important for different applications related to computing and memory devices.

Aza-CMP materials (see Fig, 1a) have a nitrogenated porous structure[11] with multiple benzene rings on a side of a hexagonal unit cell. The repeated structure results in a novel class of extended porous frameworks, which are known as π-conjugated microporous polymers. Aza-CMP[12,13], with the direct band gap of 1.65 eV[14], is promising for an electric power supply and for efficient energy storage.[15] It has been shown that the band-gap can be tuned from 1.64 to 0.96 eV by replacing hydrogens by halogen substituents varying from fluorine to iodine.[16] Indeed, the applications of the nitrogenated microporous materials are very broad. They can be useful as sensitizers in solar cells[17], for water splitting catalysis[18], in biomedicine[19], as a photocatalyst[14], and for gas storage and separation[20]. If we insert into one of the pores three locally heme-like structures we obtain the 2D crystal structure

described in Ref.[3].

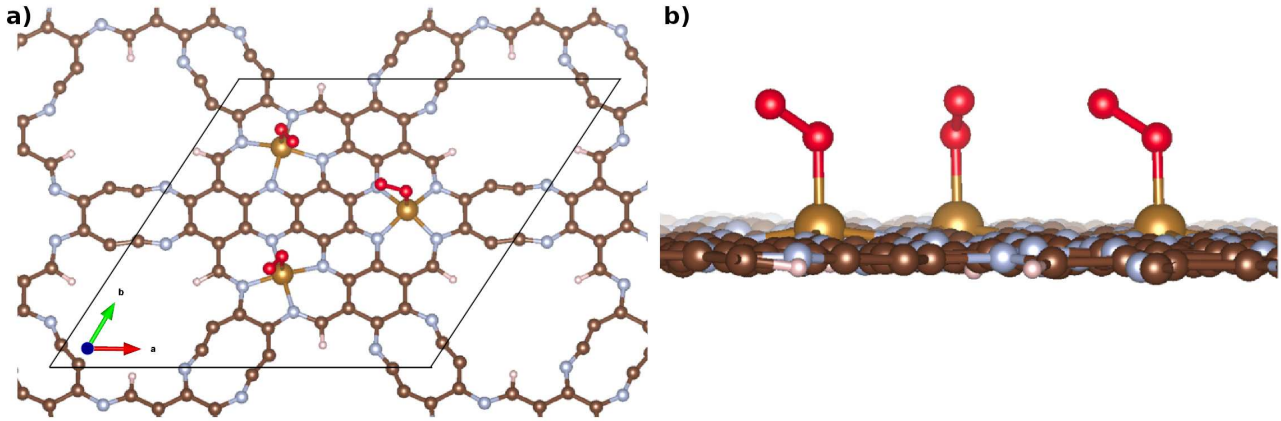

FIG. 1: Crystal structure of porphyrin-like aza-CMP with three bound O_2 molecules shown from the (a) top and (b) side. The unit cell is shown in (a). The value of the lattice constants, a and b, is 17.16 $\mathring{A}$

The purpose of this work is to investigate the impact of binding the different gaseous molecules to the iron atoms (see Fig. 1b) on the electronic, optical, electron transport, and magnetic properties of the Fe-aza-CMP. Depending on which gas molecule is bound, we see strong ferromagnetism, antiferromagnetism, and paramagnetism.

II. COMPUTATIONAL DETAILS

Physical properties of porphyrin-type aza-CMPs are investigated using first-principle electronic structure calculations. The calculations have been performed within the density functional theory (DFT) with the generalized gradient approximation (GGA) using the Vienna Ab-initio Simulation Package (VASP).[21] Projector augmented plane-wave (PAW) pseudopotentials with a cutoff energy of 400 eV have been employed for the calculations.[22]. For materials such as this, pure GGA exchange-correlation based DFT erroneously estimates magnetic properties and underestimates the band gap. To overcome this problem, we employ DFT+U with a Hubbard term of $U = 5\ eV$ which has been shown to correctly describe the magnetic and electronic properties of iron porphyrins.[23] A Γ-centered k-point grid has been generated from the Monkhorst-Pack scheme.[24] The vacuum space between

the surfaces has been chosen to be around 10 $\mathring{A}$ to avoid interaction between 2D periodic surfaces. The structure relaxation has been performed with the Pedrew-Burke-Ernzerhof (PBE) exchange-correlation functional and a $4 \times 4 \times 1$ k-mesh grid using the conjugate gradient algorithm.[25] The band structure, density of states, and absorption spectra for these materials have been calculated with a $16 \times 16 \times 1$ k-mesh grid. For the band structure calculations we have used the M-Γ-K-M path in a k-space. For the calculations along this path we have chosen 40 k-points in total. Using VASP we have calculated the frequency-dependent dielectric tensor $\varepsilon(E)$ using the independent particle approximation (IPA) to determine the absorption coefficient tensor. For magnetic calculations the exchange integral has been estimated as a difference in the ferromagnetic (FM) and anti-ferromagnetic (AFM) energies of a 2×2 super cell. The AFM configuration is made of two iron clusters with magnetic moments in the +z-direction and two iron clusters in the -z-direction. In the case of O_2 molecules the exchange integral has been verified by another independent methodology, fitting the magnon dispersion curve via the frozen magnon aproach.

III. FE-AZA-CMP WITH ATTACHED CO MOLECULES

A. Adsorption

If the Fe-aza-CMP is embedded in an CO atmosphere, there are several possibilities for molecules to be adsorbed: (a) three molecules attached to a single iron cluster (i.e. aggregated, configuration 3/0/0), (b) two molecules attached to a single cluster and one attached to another cluster (i.e. semi-aggregated, configuration 2/1/0), and (c) three molecules attached to three individual iron centers (i.e. uniform, configuration 1/1/1). Thus we ask ourselves a question, which configuration is more energetically preferable (i.e. whether all three CO molecules are attached to a single cluster, two molecules attached to one cluster and one molecule on another, or three molecules attached to three individual clusters. From the energy calculations (presented in Table I) we have found that the most preferable adsorption configurations for CO molecules are configurations 1/1/1 and 2/1/0. Configuration 3/0/0 is less energetically favorable by an energy difference of $\Delta E = 0.22\ eV$.

We have found that configurations 1/1/1 and 2/1/0 are energetically favorable.

	Distribution	Energy, eV
CO	1/1/1	-2515.35
CO	2/1/0	-2515.35
CO	3/0/0	-2515.13

TABLE I: Energies of different distributions of three bound CO molecules.

Occupation	Band Gap, eV	Magnetic Moment, μ_B	J, μeV
Single	0.269	4	28.9
Double	0.396	2	75.1
Triple	0.626	0	0.0

TABLE II: Band gap energies, magnetic moment, and exchang integral J for singly, doubly, and triply occupied CO.

B. Electronic Properties

Using the DFT+U calculations, we have found the density of state (DOS) for singly, doubly, and triply occupied Fe-aza-CMPs by CO molecules. The calculated DOS is presented in Fig. 3. If the Fe-aza-CMP is unoccupied there is a strongly localized d_{z^2} band which was studied in Ref.[3] and is presented for comparison in Fig. 2. The d_{z^2} band is visible at $E \approx 0.27\ eV$ as a narrow peak. If the Fe-aza-CMP is singly occupied, the localized band still exists with a lower intensity, however the energy gap is slightly extended. Similarly, for the doubly occupied Fe-aza-CMP the d_{z^2} band is still present with an even lower intensity with a slightly extended energy gap. For triply occupied Fe-aza-CMP, the d_{z^2} band completely disappears and the energy gap is much greater than the doublely occupied cluster as shown in Fig. 3. As we will see later, this property becomes important for light absorption. The evolution of the energy band gap with respect to the CO occupancy number is given in Table II. For the unoccupied Fe-aza-CMP we see a gap of $E = 0.27\ eV$.[3] For the singly occupied CO we see a slight reduction of the band gap to $E = 0.269\ eV$. For doubly and triply occupied Fe-aza-CMP we see a significant increase in band gap to $E = 0.396\ eV$ and $E = 0.626\ eV$, respectively.

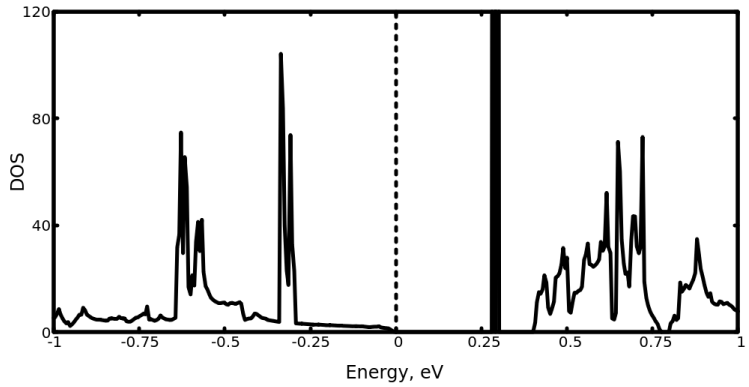

FIG. 2: Density of states (DOS) of pristine Fe-aza-CMP.

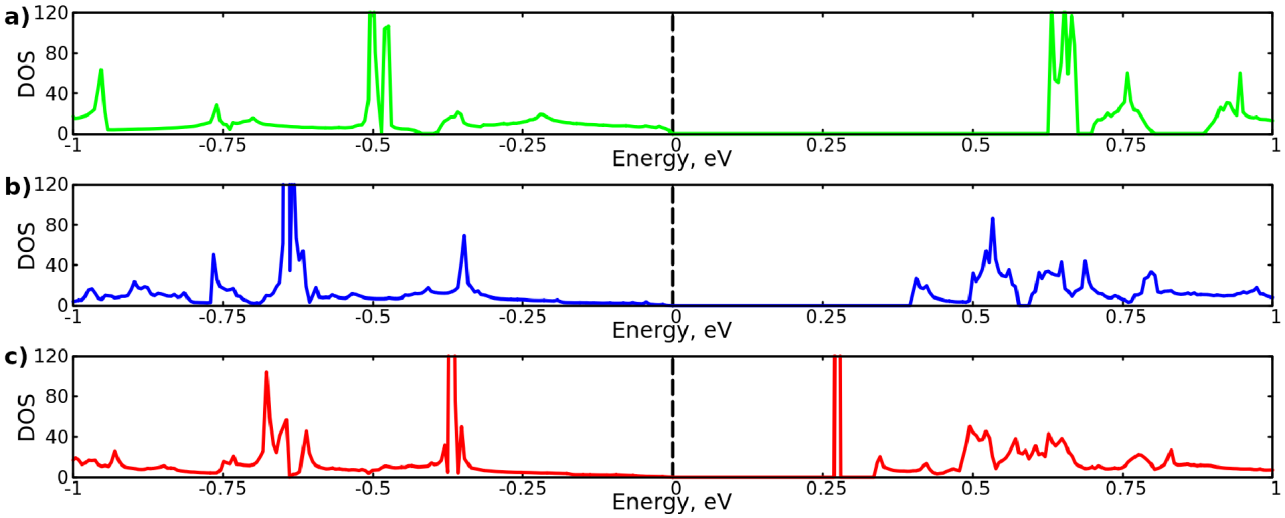

FIG. 3: Density of states (DOS) of singly (red), doubly (blue), and triply (green) occupied configurations for CO moelcules.

We would like to mention that the conduction band is modified by the presence of the CO molecules.

In addition to the DOS calculations, we have also calculated the energy band structures, presented in Fig. 4. The evolution of the band structures from singly to triply occupied Fe-aza-CMP clusters is presented in Figs. 4a, b, and c. The d_{z^2} band is shown as a straight line in the band structures. This band is a pure spin-up state as shown in Fig. 4a and b in red. The valence band for Fig. 4a are spin-down around the Γ point while the valence band for Fig. 4b is spin-up. The valence band for Fig. 4c are not spin-split. The optical

transitions between the HOMO valence band electrons in the vicinity of the Γ point are forbidden by spin for Fig. 4a and therefore takes place in k-space. However, for doubly and triply occupied Fe-aza-CMP such transitions are allowed. The electronic structure properties determine the optical absorption in such a material.

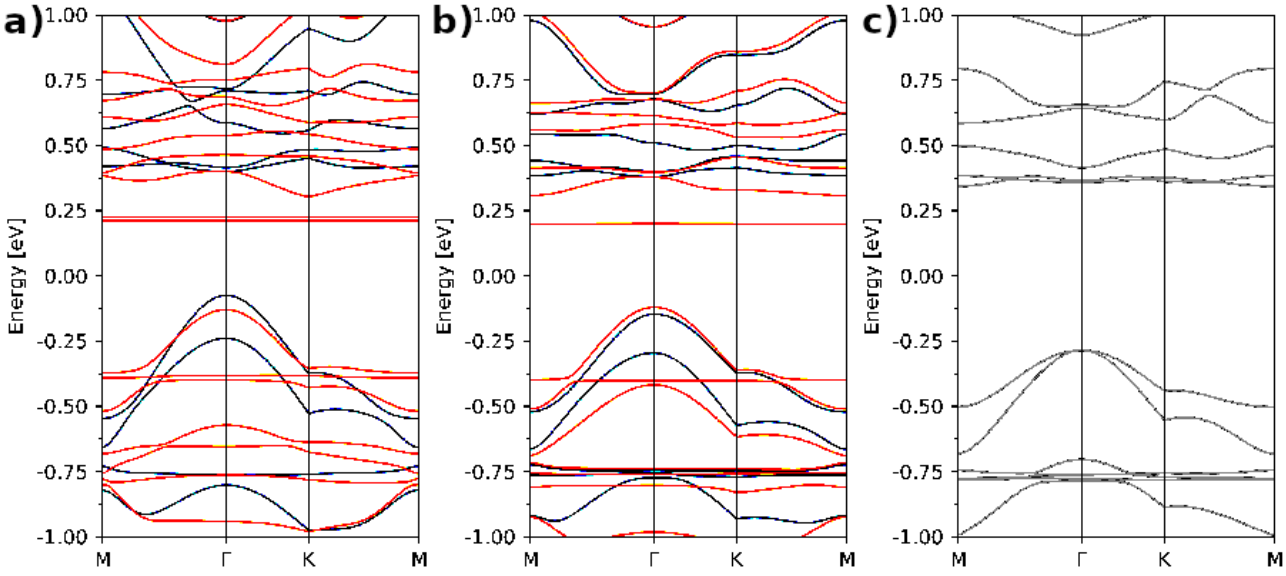

FIG. 4: Band structures for singly (a), doubly (b), and triply (c) occupied configurations for CO molecules.

C. Optical Properties

In Fig. 5 we cannot distinguish the difference in gaps due to the small amplitude modifications. However, the absorption spectrum is very different for all three cases of CO adsorption. For example, for triply occupied Fe-aza-CMP there is a strongly pronounced band at $E = 1\ eV$. Such a band exists for doubly occupied at lower amplitude and is weakly pronounced for singly occupied Fe-aza-CMP. As shown in Ref.[3], this band does not exist in the unbounded Fe-aza-CMP. Thus we conclude that occupancy of Fe-aza-CMP clusters can be determined from optical absorption experiments.

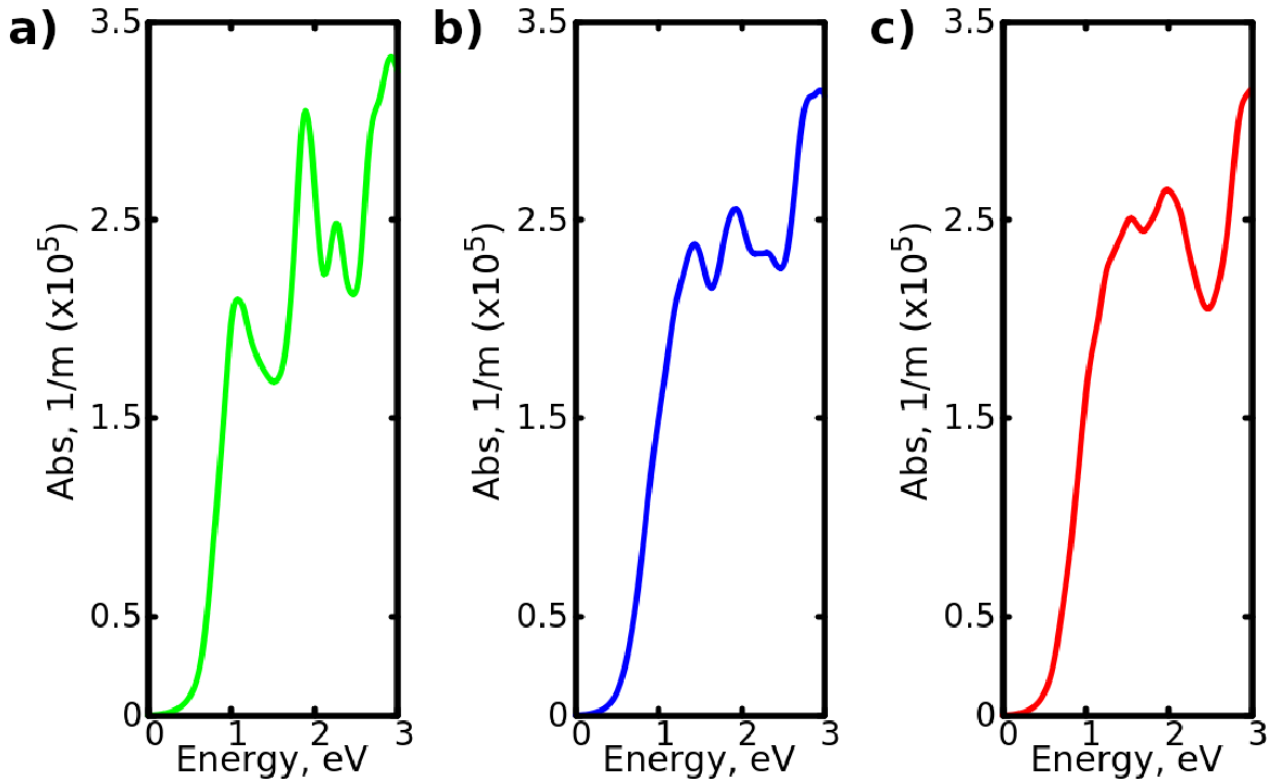

FIG. 5: Frequency dependent absorption coefficient for singly (red), doubly (blue), and triply (green) occupied configurations for CO molecules.

D. Electron Transport Properties

Electron transport properties are closely related to the absorption coefficient $\sigma(\omega) = \frac{\alpha(\omega)n(\omega)c}{4\pi}$. In Figs. 6a,b, and c, we see the evolution of $\sigma_{xx}(\omega)$, where n is the index of refraction in the direction of the conduction. In Figs. 6a, b, and c we see the evolution of $\sigma_{xx}(\omega)$. The singly and doubly occupied configurations show that the omega dependence of the conductivity is almost the same. However, for the triply occupied configuration there are more pronounced bands.

E. Magnetic Properties

In addition to electronic, optical, and electron transport properties, we have studied the magnetic properties of each CO occupancy. Pure Fe-aza-CMP is a ferromagnet with

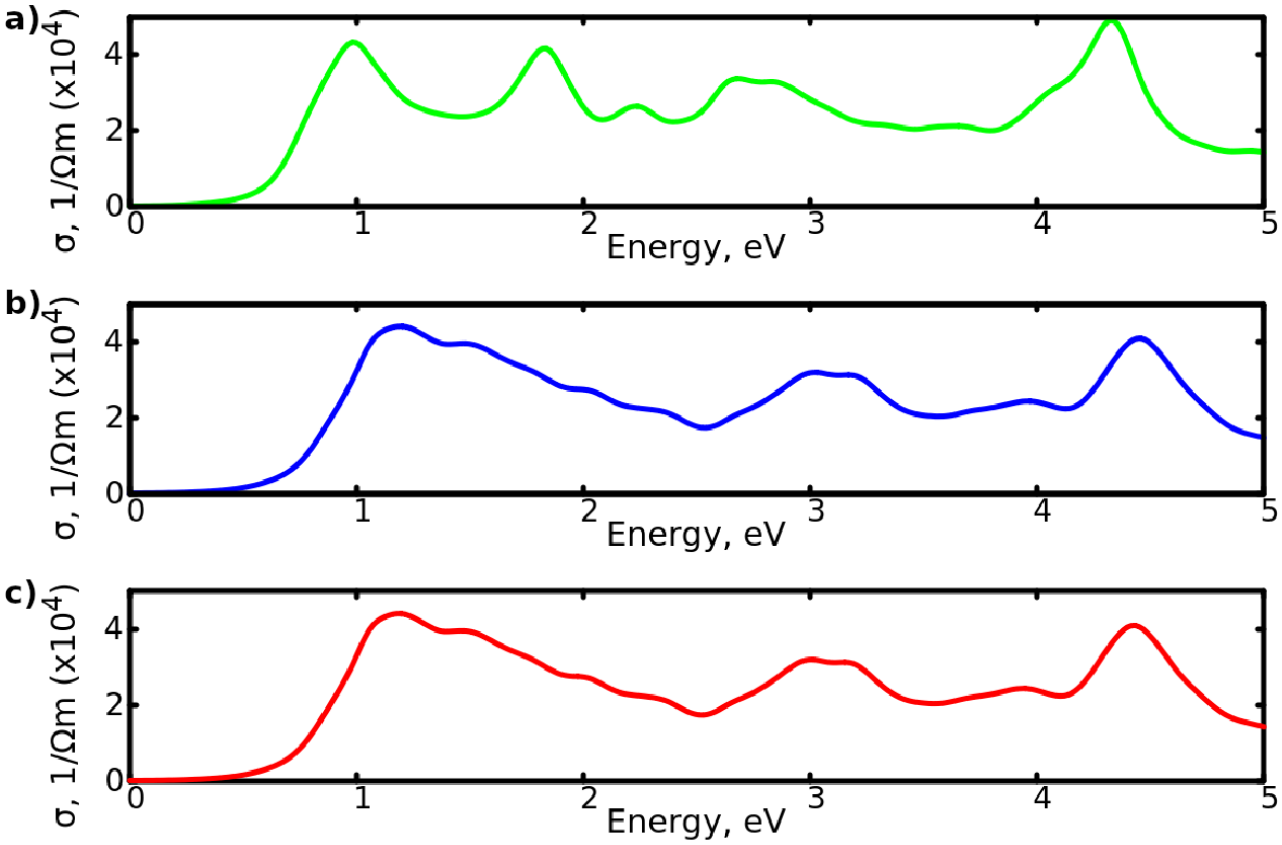

FIG. 6: Frequency dependent electrical conductivity for singly (red), doubly (blue), and triply (green) occupied configurations for CO molecules.

a magnetic moment of 6 for each iron cluster (two unpaired electrons on each iron atom). It was found that the exchange integral for pure Fe-aza-CMP is $J = 27\ \mu eV$.[3] With the CO occupation we observe decrease of the total spin for the Fe-aza-CMP iron cluster which for singly, doubly, and triply occupied are 4, 2, and 0, respectively. Therefore, triply occupied Fe-aza-CMP is non-magnetic. The exchange integral from the Ising model is presented in Table II. From the table, we can see that the adsorption of the CO molecule increases the calculated exchange integral form $J = 27\ \mu eV$ to $J = 75.1\ \mu eV$. The exchange integral has been estimated by the difference in energy between ferromagnetic (FM) and anti-ferromagnetic (AFM) states for each CO occupancy using the Ising model because of the out-of-plane magnetization. Making use of this estimation, we can identify occupation numbers and therefore, concentration of CO molecules in the system.

	Distribution	Energy, eV
CO_2	1/1/1	-2533.98
CO_2	2/1/0	-2533.91
CO_2	3/0/0	-2533.68

TABLE III: Energies of different distributions of three bound CO_2 molecules.

IV. FE-AZA-CMP WITH ATTACHED CO_2 MOLECULES

Besides CO molecules we also study the attachment of CO_2 molecules to the iron atoms in the aza-CMP crystal.

A. Adsorption

First, we analyze the adsorption of three atoms attached to the same or different iron cluster trying to understand whether a cluster aggregation or uniform distribution of CO_2 molecules is energetically favorable. From the energy calculations of different configurations of the CO_2 molecule attachments (see Table III) we have found that the most favorable attachment configuration is a single CO_2 molecule attached to a Fe-cluster and uniformly distributed over the surface. If two CO_2 molecules are attached to one Fe-cluster and one CO_2 molecule is attached to another cluster leaving one final Fe-cluster with no attachment (2/1/0) the highest energy is obtained with $\Delta E = 0.07\ eV$. The third configuration where all three CO_2 molecules are attached to one Fe-cluster leaving the other two without CO_2 molecules, has an energy difference of $\Delta E = 0.3\ eV$ from a uniform distribution. From these calculations we conclude that even at room temperature the singly occupied configuration is still favorable.

B. Electronic Properties

As shown in Ref.[3], there is a strongly localized d_{z^2} band located on the iron atoms. If one CO_2 is attached, only a small d_{z^2} band remains at $E \approx 0.26\ eV$. Another d_{z^2} band exists in the valence band which appears in the singly, doubly, and triply occupied configurations. As shown in Fig. 7b, when two CO_2 molecules are attached, the strongly localized d_{z^2} band

Occupation	Band Gap, eV	Magnetic Moment, μ_B	J, μeV
Single	0.039	4	22.6
Double	0.159	2	68.8
Triple	0.434	0	0.0

TABLE IV: Band gap energies, magnetic moment, and exchang integral J for singly, doubly, and triply occupied CO_2.

remerges again in the conduction band. For the triply occupied configuration the conduction d_{z^2} band is no longer strongly localized.

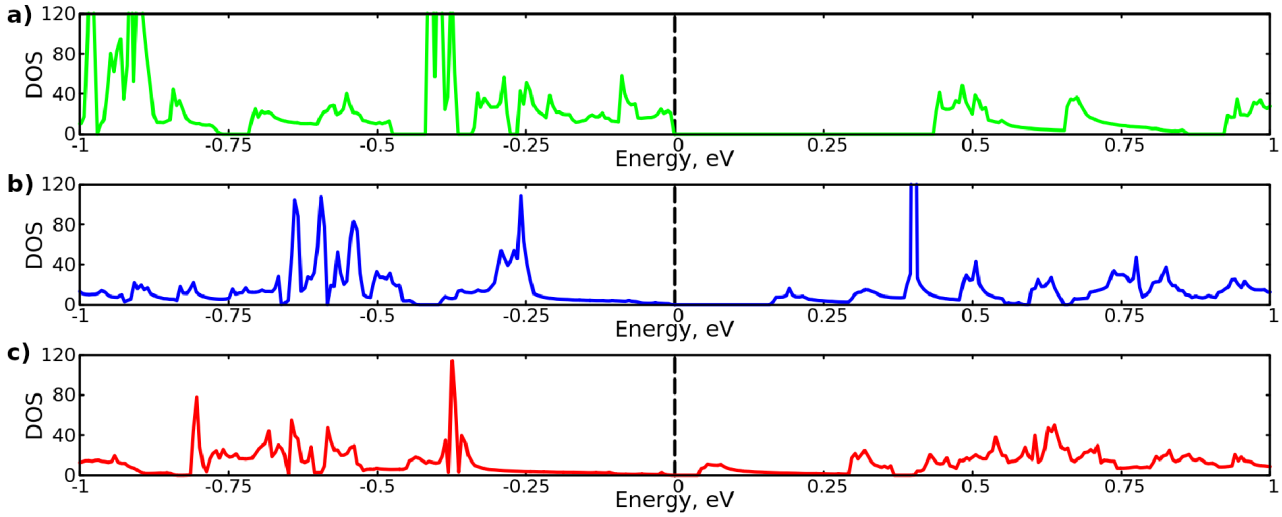

FIG. 7: Density of states (DOS) of singly (red), doubly (blue), and triply (green) occupied configurations for CO_2 moelcules.

For a single CO_2 occupation the band gap becomes extremely small, $E = 0.039\ eV$ (see Table IV). The band gap dramatically increases for doubly and triply occupied to $E = 0.159\ eV$ and $E = 0.434\ eV$, respectively. In addition, we have studied the band structures for the three cases where one, two, and three CO_2 molecules are bound to the iron atoms. From Figs. 8a, b, and c where the band structures are presented for singly, doubly, and triply occupied configurations we see that the band-gaps are indirect. The valence band maximum is at the Γ point while the conduction band minimum is at the M point. For a single CO_2 molecule attachment we see the strongly localized d_{z^2} band located outside of the gap contrary to the CO attachment where the band is within the gap. The

conduction and valence bands are for spin-down occupations only. For the triply occupied configuration we see no spin splitting and all the bands are doubly degenerate.

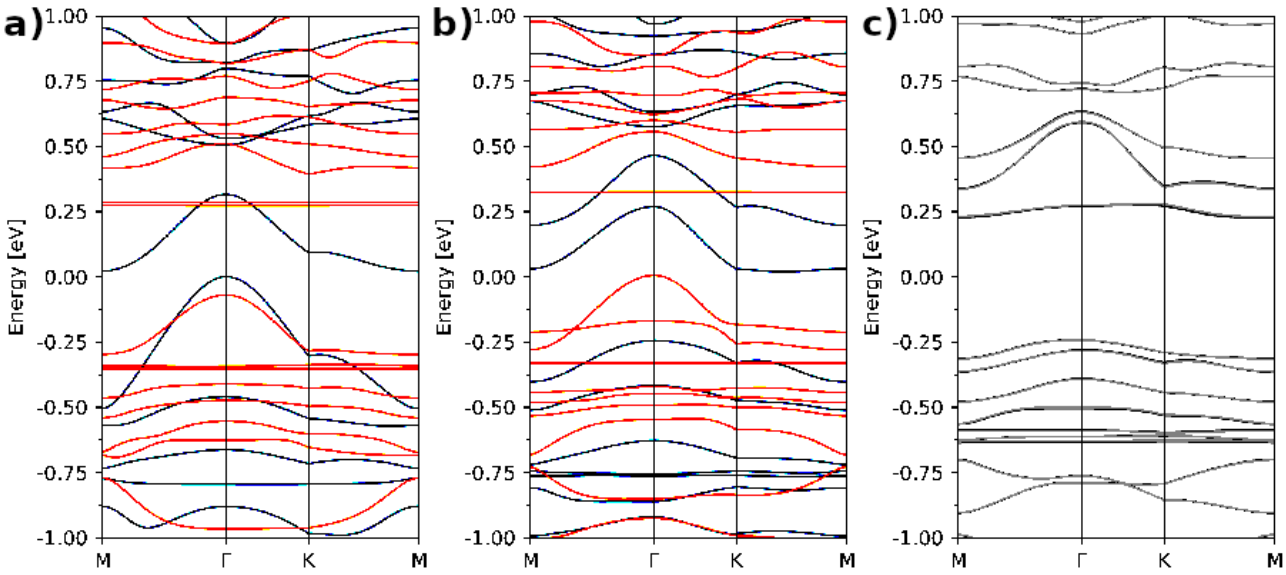

FIG. 8: Band structures for singly (a), doubly (b), and triply (c) occupied configurations for CO_2 molecules.

C. Optical Properties

We have also studied the optical absorption coefficients for the singly, doubly, and triply occupied configurations of the Fe-aza-CMP by CO_2 molecules. The absorption spectra is presented in Figs. 9a, b, and c. The absorption spectra are different for all three cases. The d_{z^2} band is strongly pronounced for the doubly occupied configuration. This peak is much less pronounced for the singly and triply occupied configurations. For the triply occupied configuration, there is a shoulder at $E = 1\ eV$.

D. Electron Transport Properties

The frequency-dependent electrical conductivity is closely related to the absorption spectrum and is presented for all three occupation configurations of CO_2 in Fig. 10. Because of the frequency-dependence of the refractive index, the frequency dependence of the electrical

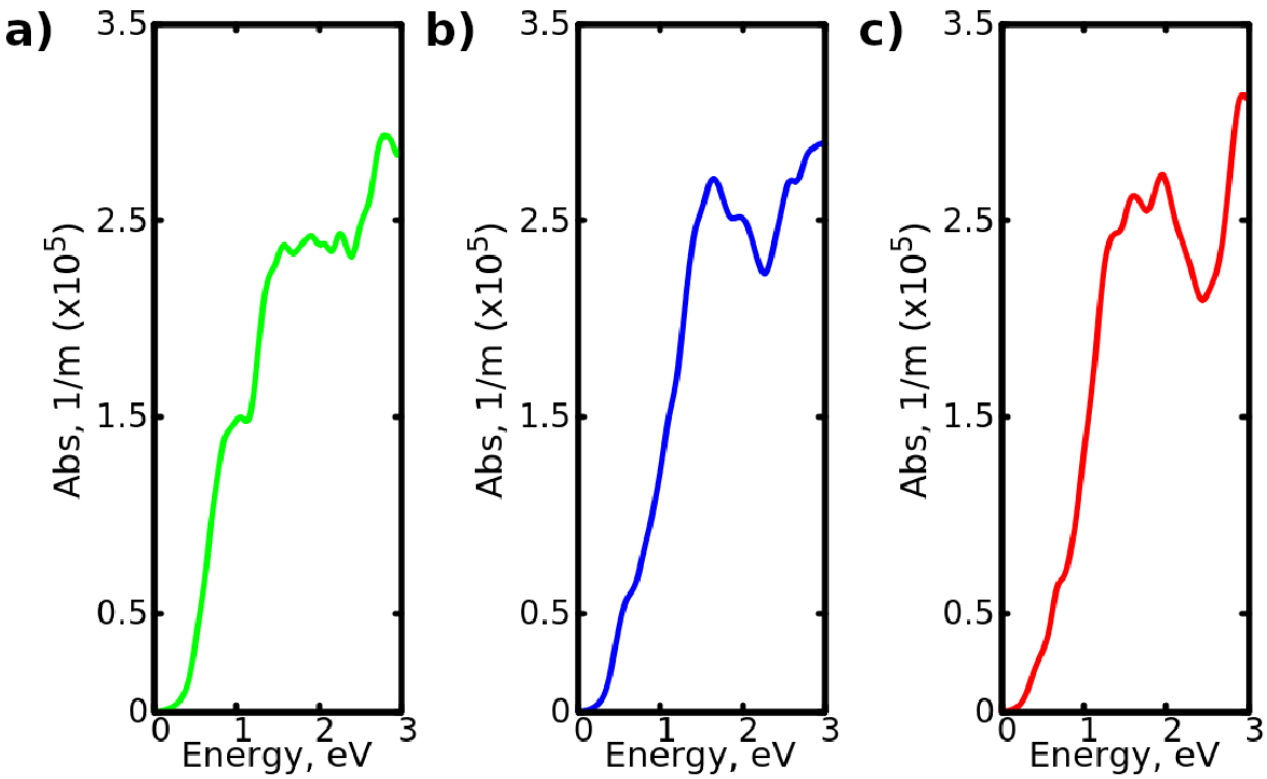

FIG. 9: Frequency dependent absorption coefficient for singly (red), doubly (blue), and triply (green) occupied configurations for CO_2 molecules.

conductivity is not the same of the absorption coefficient. The frequency-dependent electrical conductivity for singly, doubly, and triply occupied configurations for CO2 molecules are very close to each other. However, for the singly occupied configuration there is a small shoulder at lower energies.

E. Magnetic Properties

As shown in Ref.[3], the Fe-aza-CMP exhibits ferromagnetism with iron clusters having M = 6. If we attach one, two, or three CO_2 molecules to the Fe-aza-CMP we see the gradual decrease of the magnetic moment to 4, 2, and 0 respectively. Thus, in the presence of CO_2 the total magnetic moment of the Fe-aza-CMP changes similar to the case of CO. In the case of triple occupation the Fe-aza-CMP becomes paramagnetic. We also studied the exchange integrals for the Ising model and found that the exchange integral is slightly smaller than that of the CO case. For singly and doubly occupied configurations the exchange integrals

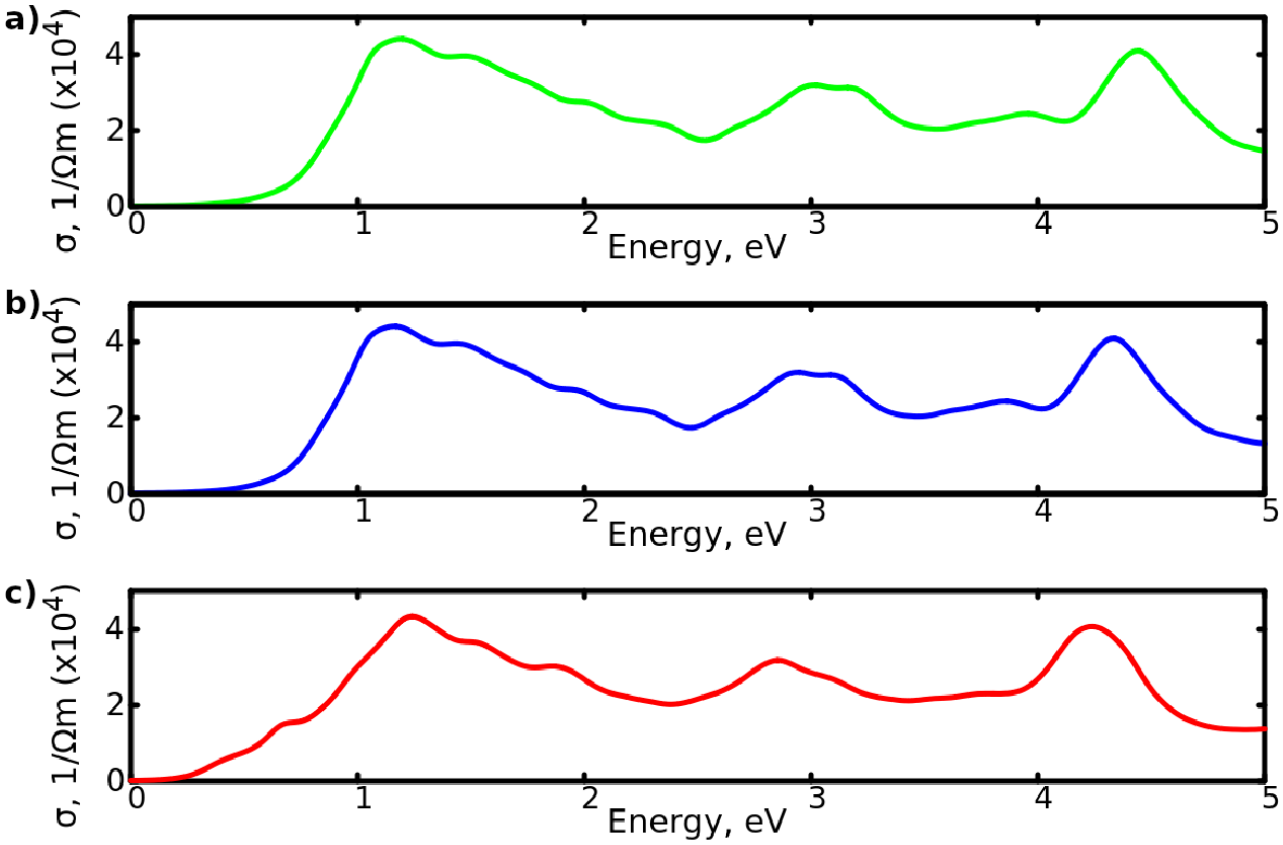

FIG. 10: Frequency dependent electrical conductivity for singly (red), doubly (blue), and triply (green) occupied configurations for CO_2 molecules.

become 22.6 μeV and 68.8 μeV respectively as shown in Table IV.

V. FE-AZA-CMP WITH ATTACHED O_2 MOLECULES

A. Adsorption Properties

We have studied the binding energies of a single molecule of CO, CO_2, and O_2 and found that the highest binding energy is for CO_2, $E = -1.340\ eV$, CO has slightly lower binding energy, $E = -1.324\ eV$, while O_2 has a value of nearly half, $E = -0.786\ eV$. In order to understand how O_2 molecules distributes among the clusters we studied the following configurations: three molecules attached to three different iron clusters (configuration 1/1/1), another configuration where two molecules are on one iron cluster with one molecule attached

	Distribution	Energy, eV
O_2	1/1/1	-2498.79
O_2	2/1/0	-2499.16
O_2	3/0/0	-2499.15

TABLE V: Energies of different distributions of three bound O_2 molecules.

Occupation	Band Gap, eV	Magnetic Moment, μ_B	J, μeV
Single	0.303	4	-144.5
Double	0.291	2	1071.9
Triple	0.347	0	0.0

TABLE VI: Band gap energies, magnetic moment, and exchang integral J for singly, doubly, and triply occupied O_2.

to a different cluster (configuration 2/1/0), and a configuration where all three molecules are attached to the same iron cluster (configuration 3/0/0). From the energy calculations (presented in Table V) we have found that O_2 prefers the aggregation of molecules in configuration 2/1/0 or 3/0/0 with almost no energy difference, 0.01 eV, which is almost negligible for room temperatures. The uniform distribution, configuration 1/1/1, has a much higher energy, $\Delta E = 0.36\ eV$. Thus such aggregation might be important for practical purposes when we consider the magnetic properties of O_2 Fe-aza-CMPs. These aggregations might be practical for applications of the magnetic properties of O_2 bounded Fe-aza-CMPs.

B. Electronic Properties

In Fig. 11 we present the results of the calculations of the DOS for the three cases of O_2 occupation of the iron clusters. We see the d_{z^2} band is strongly pronounced in the conduction band for all three cases. The band gaps values are slightly changed. Indeed for singly occupied $E = 0.303\ eV$, for doubly $E = 0.291\ eV$, and for triply $E = 0.347\ eV$ (see Table VI). It is interesting to note, that for the doubly occupied configuration the band gap slightly shrinks in contrast to CO and CO_2 cases where the monatomic dependence have been observed.

In addition to the DOS, we have also caculated the band structures for all three O_2

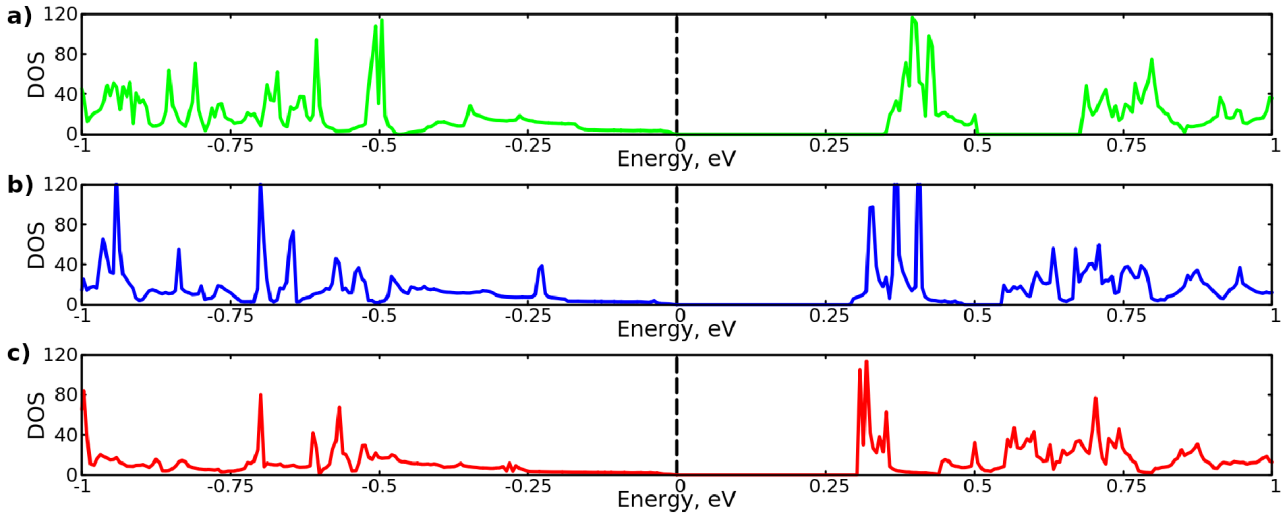

FIG. 11: Density of states (DOS) of singly (red), doubly (blue), and triply (green) occupied configurations for O_2 moelcules.

occupation confiugrations (see Fig. 12) and have found very interesting features despite the similar band gap values. Indeed, the d_{z^2} localized band in the valence is strongly present for the single occupation, is much less pronounced for the double occupation, and does not exist in the triply occupied case. The HOMO valence band has interesting spin dependent properties. Indeed, for the Γ- and K-points it is determined by spin-down electrons for singly and doubly occupied cases and in the vicinity of M points it is completely described by the d_{z^2} band. The contribution of states in the vicinity of the Γ point vanishes, however, for larger k-vectors is allowed. For the triply occupied case the situation is completely different. The HOMO band is doubly degenerate at the Γ point and is determined by spin-up electrons. For all occupation cases the minimum of the conduction band is at the K point. The transition from the valence band maximum and conduction band minimum is forbidden by the spin selection rules.

C. Optical Properties

We have also studied the optical properties of singly, doubly, and triply occupied O_2 configurations, presented in Fig. 13. The absorption for all three occupation cases are similar to each other and probably cannot be used to determine an occupation state of

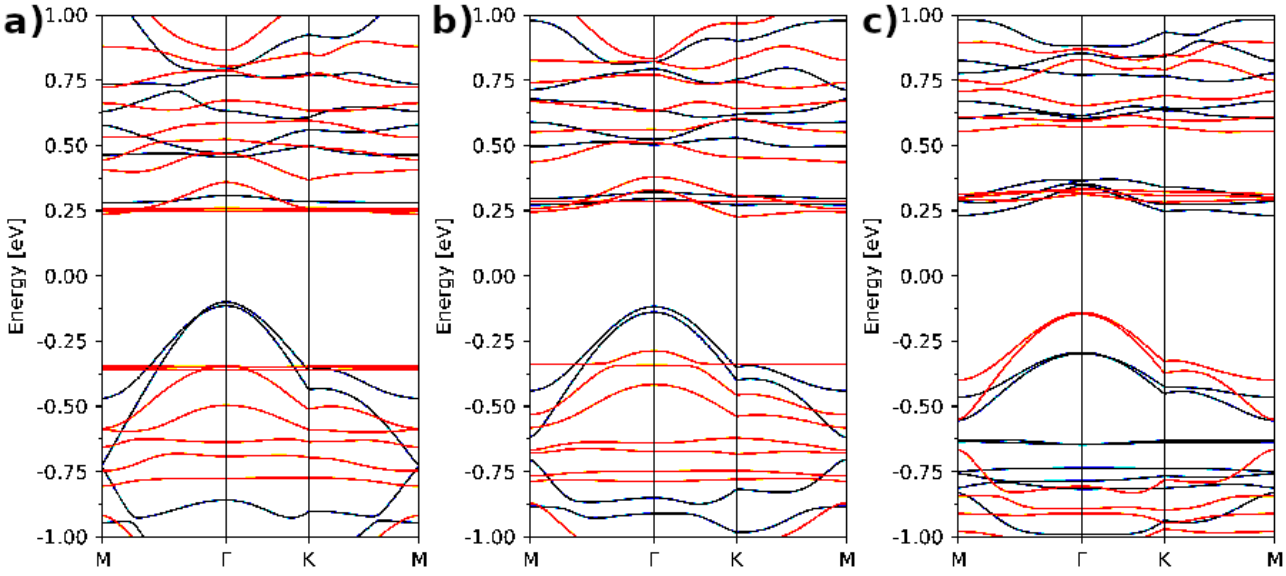

FIG. 12: Band structures for singly (a), doubly (b), and triply (c) occupied configurations for O_2 molecules.

O_2 molecules. Indeed, we observe a strong absorption band at 1.3 eV. We would like to mention that many transitions in k-space are forbidden by spin in the vicinity of the Γ-point. However, for larger k-vectors they are allowed. Such a physical situation decreases the number of states participating in absorption.

D. Electron Transport Properties

The electrical conductivity, σ_{xx} or σ_{yy} should resemble the absorption coefficient corrected by the frequency dependent refractive index. For Figs. 14a, b, and c we see that all three O_2 occupation cases are very similar. A strong electrical conductivity is observed at the value of 1.3 eV, similar to the optical absorption coefficients for all three cases. This similarity between the peaks of the electrical conductivity and the optical absoprtion is an interesting result worthy of investigation but is beyond the scope of this work.

E. Magnetic Properties

The magnetic properties for the three O_2 occupations are very different than CO and CO_2 attachment configurations as shown in Table VI. The value of the magnetic moment

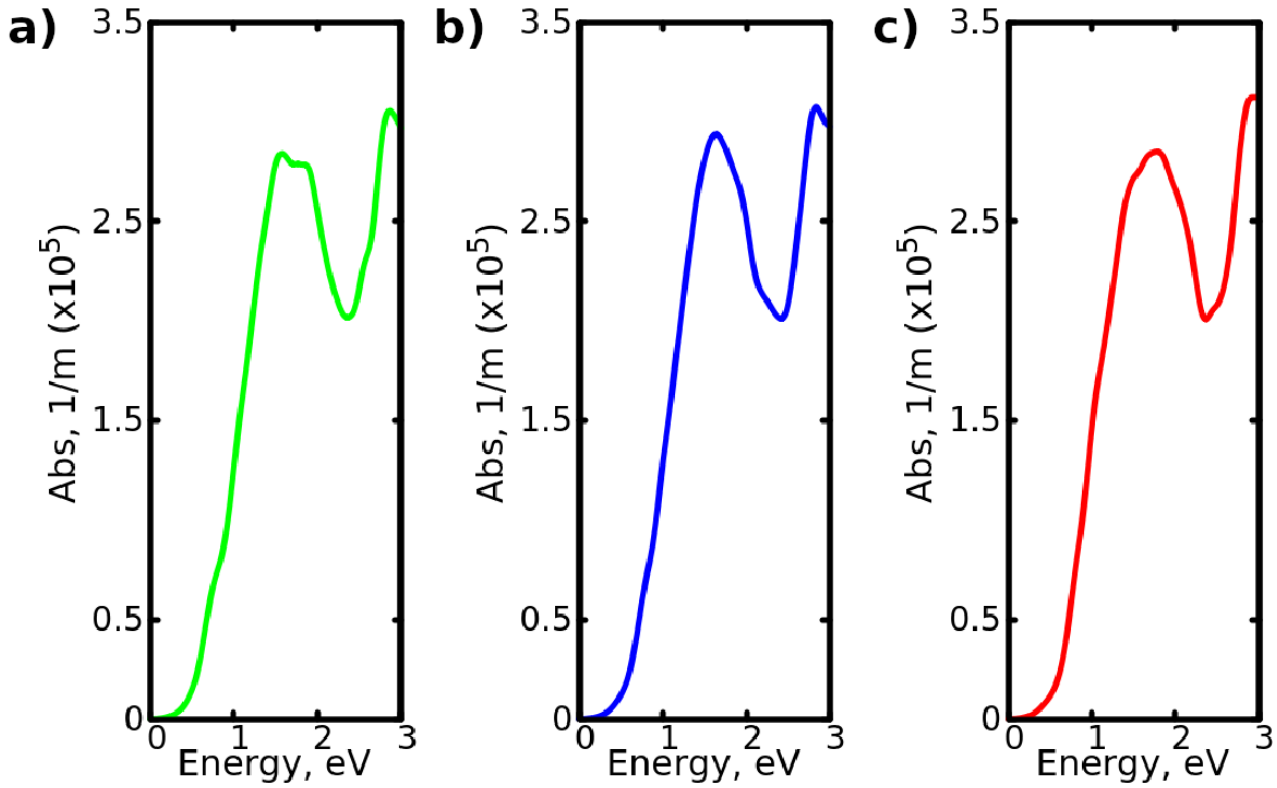

FIG. 13: Frequency dependent absorption coefficient for singly (red), doubly (blue), and triply (green) occupied configurations for O_2 molecules.

for individual clusters decreases from 4 to 0 with the O_2 occupation number. However, the exchange integral for a single O_2 occupation indicates an antiferromagnetic nature of the magnetic state. If the iron cluster is doubly occupied the magnetic state is ferromagnetic with an extremely large exchange integral of $J = 1071.9\ \mu eV$. For triple O_2 occupation of the Fe-aza-CMP clusters we have found a paramagnetic state with S = 0. The case for double occupation of the Fe-aza-CMP has a high exchange integral which indicates high values for the Curie temperature. Indeed, we have estimated the Curie temperature for this case and have found $T_c \approx 200\ K$. Our research has been focused on this specific case and we have verified the exchange constant using an independent method to calculate the exchange integral. In particular, we have conducted the frozen magnon approached for this configuration described by:

$$\Delta E_{Magnon} = 2M[6J_{NN} - J_{NN}\Sigma_{\vec{q}} cos(\vec{q} \cdot \vec{R_{NN}})]$$

where J_{NN} is the nearest-neighbor exchange integral, M is the cluster magnetic moment,

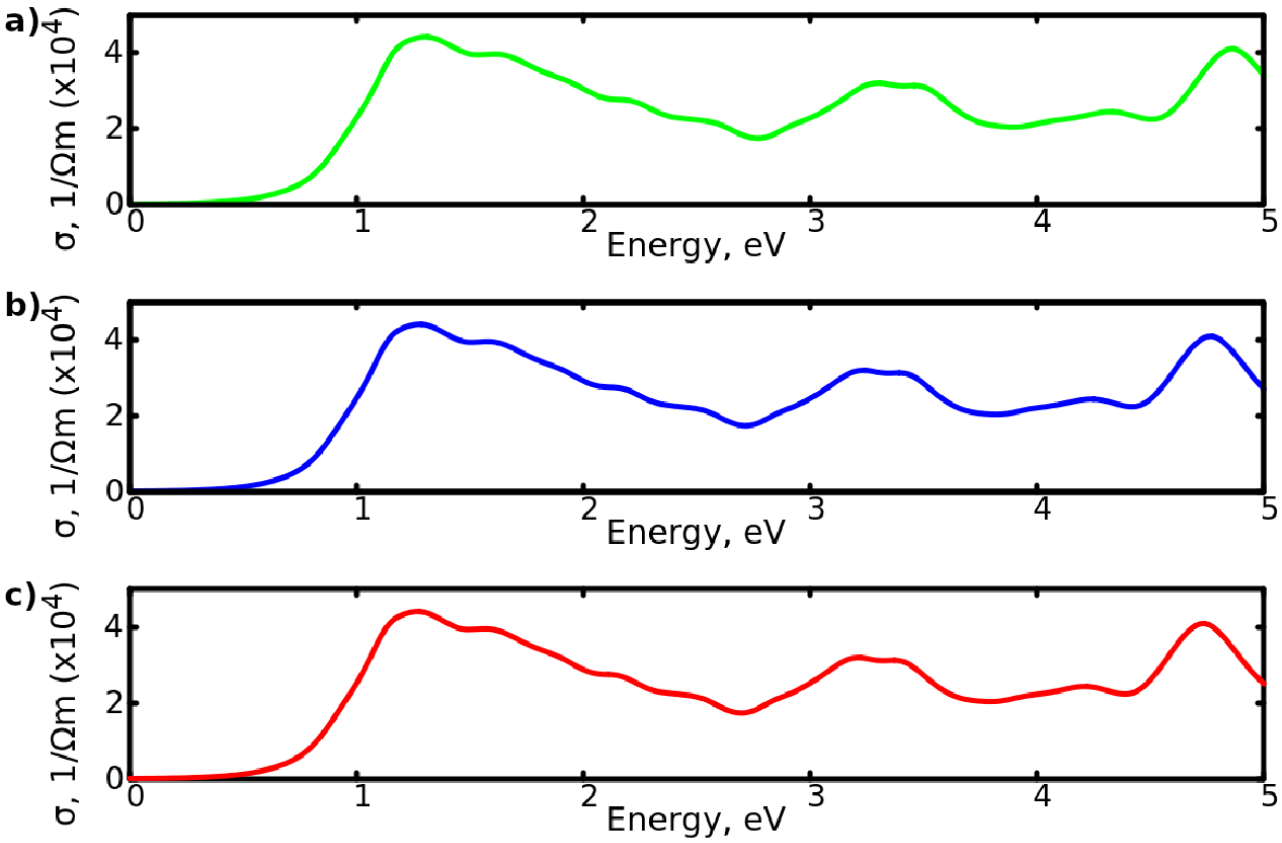

FIG. 14: Frequency dependent electrical conductivity for singly (red), doubly (blue), and triply (green) occupied configurations for O_2 molecules.

$\vec{q}$ is the magnon vector such that $\vec{q} = \frac{2\pi}{a_0} \cdot Q$, and $\vec{R_{NN}}$ is the position of the nearest-neighbor. The fitting of the above equation to the calculated magnon dispersion curve is presented in Fig. 15. We have found that the best fit for the exchange integral value is $J = 1016\ \mu eV$. This is very close to the estimation of the exchange integral by the difference in energies of the ferromagnetic and antiferromagnetic states.

VI. CONCLUSIONS

In this work we have studied adsorption, electronic, optical, electron transport, and magnetic properties of CO, CO_2, and O_2 molecules attached to iron atoms in 2D ferromagnetic aza-CMPs. We have considered single, double, and triple attachments of each type of molecules to the 2D crystal. The binding energies are -1.324, -1.34, and $-0.786\ eV$

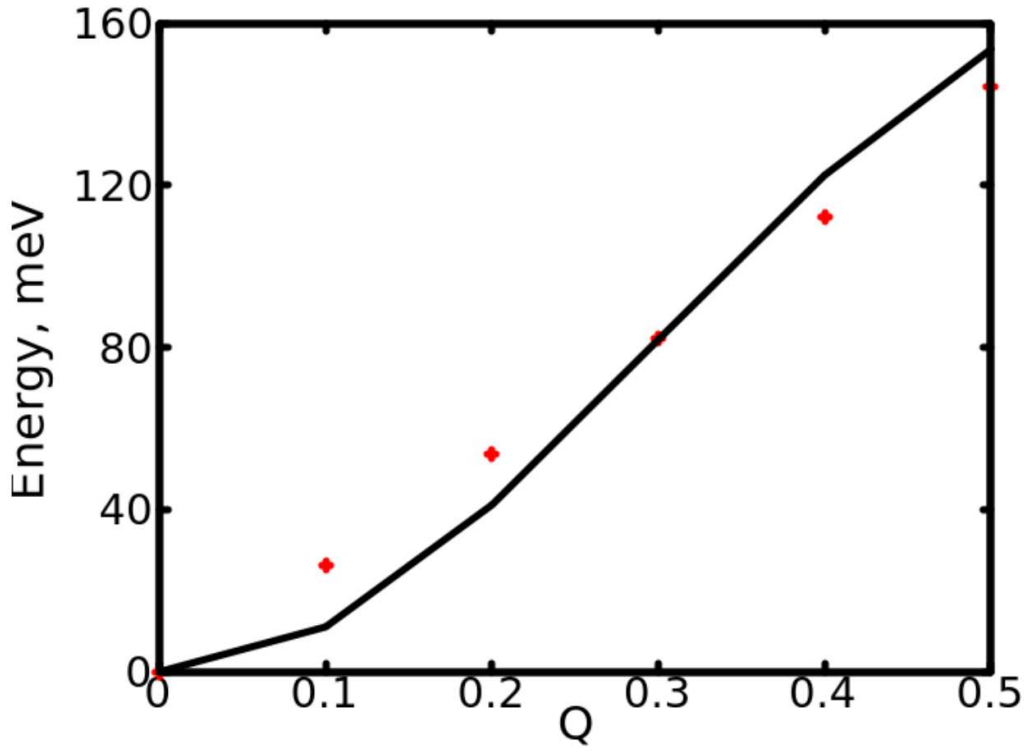

FIG. 15: Magnon dispersion for doubly occupied configuration of O_2 molecules.

for CO, CO_2, and O_2 respectively. If the adsorption takes place from a gaseous atmosphere the most likely attachment to the Fe-aza-CMP surface is uniform distribution for CO and CO_2 (see Tables I and III) and aggregation for O_2 (see Table V). The electronic band structure and density of states show a strong d_{z^2} band from the iron atoms for a singly and doubly occupied configurations and disappears for the triply occupied case. The absorption coefficient is almost the same for singly, doubly, and triply occupied configurations for each molecule. From Figs. 6,10, and 14 we conclude that the frequency dependence of the electrical conductivities is similar for each occupation number for each molecule and therefore cannot be used to determine the level of occupation of molecules on the Fe-aza-CMP iron cluster. The magnetic properties are the most interesting in this research. For all three gas molecules the magnetic moment decreases from 4 to 2 to 0 when single, double, or triple molecules are attached to the Fe-aza-CMP. The most interesting case is an O_2 molecule. When two O_2 molecules are attached to a Fe-aza-CMP there is a very large exchange integral, $J = 1.1\ meV$ (see Table VI). Such a large value of J leads to a high Curie temperature

that is $T_c \approx 200\ K$. To make sure that the value of J is correctly calculated we have used two independent methodologies where in the first case the exchange integral has been found from the energy difference between ferromagnetic and antiferromagnetic configurations. The second method used to find J is the frozen magnon approach. From the first method we found $J = 1071\ \mu eV$ and from the second $J = 1100\ \mu eV$. In addition, we would like to mention that an antiferromagnetic state is observed for singly occupied O_2 attachment with $J = -78.2\ \mu eV$ (see Table VI).

The results found in this work are important for 2D ferromagnetism in which the Curie temperature is very high. Fe-aza-CMPs are non-toxic and thereby can be broadly used for different applications. As the prototypes of hemoglobin and myoglobin they can be used for medical purposes in research which studies biological activities. In addition, the long range ferromagnetic ordering has applications in spintronics and other magnetic technological applications.

Acknowledgments

This work was supported by a grant from the U S National Science Foundation (No. DMR-1710512) and the U S Department of Energy (No. DE-SC0020074) to the University of Wyoming.

[1] K. S. Novoselov, A. K. Geim, S. V. Morozov, D. Jiang, Y. Zhang, S. V. Dubonos, I. V. Grigorieva, and A. A. Firsov, *Science*, 2004, **306**(5696), 666–669.

[2] M. Xu, T. Liang, M. Shi, and H. Chen, *Chemical Reviews*, 2013, **113**(5), 3766–3798.

[3] A. Pimachev, R. D. Nielsen, A. Karanovich, and Y. Dahnovsky, *Physical Chemistry Chemical Physics*, 2019.

[4] C. Gong, L. Li, Z. Li, H. Ji, A. Stern, Y. Xia, T. Cao, W. Bao, C. Wang, Y. Wang, et al., *Nature*, 2017, **546**(7657), 265.

[5] B. Huang, G. Clark, E. Navarro-Moratalla, D. R. Klein, R. Cheng, K. L. Seyler, D. Zhong, E. Schmidgall, M. A. McGuire, D. H. Cobden, et al., *Nature*, 2017, **546**(7657), 270.

[6] C. Ataca, H. Sahin, and S. Ciraci, *The Journal of Physical Chemistry C*, 2012, **116**(16), 8983–

8999.

[7] X. Li and J. Yang, *Journal of Materials Chemistry C*, 2014, **2**(34), 7071–7076.

[8] H. L. Zhuang, Y. Xie, P. Kent, and P. Ganesh, *Physical Review B*, 2015, **92**(3), 035407.

[9] W.-B. Zhang, Q. Qu, P. Zhu, and C.-H. Lam, *Journal of Materials Chemistry C*, 2015, **3**(48), 12457–12468.

[10] M. Yu, X. Liu, and W. Guo, *Physical Chemistry Chemical Physics*, 2018, **20**(9), 6374–6382.

[11] M. Bieri, M. Treier, J. Cai, K. Aït-Mansour, P. Ruffieux, O. Gröning, P. Gröning, M. Kastler, R. Rieger, X. Feng, K. Müller, and R. Fasel, *Chem. Commun.(Cambridge)*, 2009, **45**, 6919.

[12] Z.-D. Yang, W. Wu, and X. C. Zeng, *Journal of Materials Chemistry C*, 2014, **2**(16), 2902–2907.

[13] V. Briega-Martos, A. Ferre-Vilaplana, A. de la Pena, J. L. Segura, F. Zamora, J. M. Feliu, and E. Herrero, *ACS Catalysis*, 2016, **7**(2), 1015–1024.

[14] L. Wang, Y. Wan, Y. Ding, Y. Niu, Y. Xiong, X. Wu, and H. Xu, *Nanoscale*, 2017, **9**(12), 4090–4096.

[15] Y. Kou, Y. Xu, Z. Guo, and D. Jiang, *Angewandte Chemie*, 2011, **123**(37), 8912–8916.

[16] A. Pimachev, V. Proshchenko, and Y. Dahnovsky, *Journal of Applied Physics*, 2017, **122**(11), 115305.

[17] S. Fukuzumi, Y.-M. Lee, and W. Nam, *Chemistry–A European Journal*, 2018, **24**(20), 5016–5031.

[18] L. Wang, X. Zheng, L. Chen, Y. Xiong, and H. Xu, *Angewandte Chemie International Edition*, 2018, **57**(13), 3454–3458.

[19] T. T. Lee and R. L. Momparler, *Analytical Biochemistry*, 1976, **71**(1), 60–67.

[20] A. Pimachev and Y. Dahnovsky, *Journal of Applied Physics*, 2018, **124**(19), 194303.

[21] G. Kresse and J. Furthmüller, *Computational Materials Science*, 1996, **6**(1), 15–50.

[22] P. E. Blöchl, *Physical Review B*, 1994, **50**(24), 17953–17979.

[23] D. A. Scherlis, M. Cococcioni, P. Sit, and N. Marzari, *The Journal of Physical Chemistry B*, 2007, **111**(25), 7384–7391.

[24] H. J. Monkhorst and J. D. Pack, *Physical Review B*, 1976, **13**(12), 5188.

[25] J. P. Perdew, K. Burke, and M. Ernzerhof, *Physical Review Letters*, 1996, **77**(18), 3865–3868.